Technical Report

TR-99-39

Influence of phosphorous and sulphur as well as grain size on creep in pure copper

Henrik Andersson, Facredin Seitisleam, Rolf Sandström,
Swedish Institute for Metals Research

December 1999

Svensk Kärnbränslehantering AB
Swedish Nuclear Fuel
and Waste Management Co
Box 5864
SE-102 40 Stockholm Sweden
Tel 08-459 84 00
+46 8 459 84 00
Fax 08-661 57 19
+46 8 661 57 19

Influence of phosphorous and sulphur as well as grain size on creep in pure copper

Henrik Andersson, Facredin Seitisleam, Rolf Sandström,
Swedish Institute for Metals Research

December 1999

Abstract

Uniaxial creep tests have been performed at 175 °C for extruded oxygen-free copper. The effect of different contents of phosphorous and sulphur as well as different grain sizes have been studied. The copper with <1 ppm phosphorous and with a 6 ppm sulphur content showed significantly lower creep life and ductility than batches with higher P content. An increase of the P content to 29 ppm increased the creep life and ductility, but a further increase did not affect the properties further. A similar drop in the creep properties was found in the material with a grain size of about 2000 μm. A reduction of the mean grain size to 800 μm had a beneficial effect on the creep ductility. A further reduction of the grain size did not give any further improvements. All tests except those with a phosphorous content of less than 1 ppm P and those with a mean grain size of about 2000 μm failed at an elongation greater than 20%, most of them at 30–40%. The variation in sulphur content from 6 to 12 ppm did not affect the creep properties. The main creep rupture mechanisms were found to be cavitation and microcracking at the grain boundaries. Master curves for extrapolation are provided for creep rupture as well as for 5% and 10% creep strain.

Sammanfattning

Enaxliga kryptester har utförts vid 175 °C på extruderad syrefri koppar. Inverkan av olika halter av såväl fosfor och svavel som olika kornstorlek har studerats. Kopparn med <1 ppm fosfor och med en svavelhalt på 6 ppm visade signifikant lägre kryplivslängd och krypduktilitet än satser med högre P-innehåll. En ökning av P-innehållet till 29 ppm ökade kryplivslängden och krypduktiliteten, men en ytterligare ökning påverkade inte egenskaperna ytterligare. En liknande sänkning av krypegenskaperna observerades i materialet med en kornstorlek på omkring 2000 μm. En minskning av medelkornstorleken till 800 μm hade en gynnsam inverkan på krypduktiliteten. En ytterligare minskning av kornstorleken gav inga ytterligare förbättringar. Alla tester utom de med en fosforhalt mindre än 1 ppm P och de med en medelkornstorlek på omkring 2000 μm gick till brott vid en förlängning större än 20%, de flesta vid 30–40%. Variationen i svavelinnehåll från 6 till 12 ppm påverkade inte krypegenskaperna. Huvudmekanismen för krypbrott befanns vara kavitation och mikrosprickor vid korngränserna. Masterkurvor för extrapolation presenteras för såväl krypbrott som 5% och 10% kryptöjning.

Table of contents

1 Introduction

Spent nuclear fuel in Sweden is planned to be disposed of by encapsulation in double-walled canisters consisting of iron and copper, respectively, and placed at a depth of about 500 m in the bedrock. The inner iron container is designed to carry the load and has a minimum wall thickness of 50 mm. The main function of the outer copper canister is to provide corrosion resistance. The wall thickness of this component is also 50 mm /1-1/. The copper canister will have an outer diameter of about 1050 mm, a height of about 5000 mm. The gap between the inner and the outer shells is 1–2 mm. When the canister is exposed to a slowly increasing external hydrostatic pressure, this gap will close due to creep in the copper. The maximum strain is estimated to 4%.

The temperature of the canisters due to the nuclear reactions within the spent fuel is estimated to be about 80–90 °C during the first 100–200 years in the repository. Then the temperature will gradually decrease to that of the surrounding rock, 15 °C, during the first thousand years of containment /1-1/. It is during this period that creep deformation of the copper (about 4%) is expected to occur and it is therefore important that the copper has adequate creep ductility.

The creep properties of pure coppers have been studied previously. A review of the creep properties of oxygen-free high conductivity copper (Cu-OFHC) is given in /1-2/. Oxygen-free copper with about 50 ppm phosphorous (Cu-OFP) is covered in three reports /1-3 – 1-5/. Of the two materials the Cu-OFP exhibited significantly higher creep strength and ductility. Both the Cu-OFHC and the Cu-OFP contain trace amounts of sulphur. At sulphur levels of 10 ppm the creep ductility of Cu-OFHC fell to less than 1% at temperatures above 160ºC /1-2/. When the S level was reduced to 6 ppm in the Cu-OFHC with a grain size of 50 µm, the creep ductility increased to about 10%. For coppers with about 50 ppm P the creep ductility was about 40%.

One of the methods considered for the manufacturing of the copper canisters is extrusion /1-6/. Trial production performed has indicated it to be a feasible method, however the observed grain sizes have sometimes been large. This may give problems with the creep ductility. Furthermore the large size of the canisters means that large variations in grain size within the same canister may occur.

The aim of this work is to study the effect of phosphorus, sulphur content and grain size on the creep properties of pure copper. Parallel to this work, investigations have been performed on the recrystallization and extrusion properties of copper with the same chemical composition as in this investigation. These investigations have been reported in /1-7, 1-8/.

2 Experimental

2.1 Material

Outokumpu Poricopper OY, FINLAND extruded the material used in this investigation and the composition and grain size can be found in Table 2-1. Outokumpu determined the grain sizes with the help of a reference scale /2-1/. Twinning is not included in the grain size listed in Table 2-1. The materials are designated CuP*(phosphorus content in ppm*)_(*grain size in µm*). In materials 1 (CuP0_300), 2 (CuP30_450), 3 (CuP60_350) and 4 (CuP105_450), the phosphorus content is varied. In materials 3 (CuP60_350) and 5 (CuP65_450) the sulphur content is different and finally in materials 6 (CuP60_100), 3 (CuP60_350), 7 (CuP60_800) and 8 (CuP60_2000) the grain size is changed. Material number 3 (CuP60_350) is common to all the creep test series and was used as a reference. The material was delivered in the form of 1000 to 1500 mm long rods with a diameter of 16 mm. The tensile properties and the hardness of the batches at room temperatures are listed in Table 2-2. These properties are very close for the different batches. The materials follow essentially the UNS specifications of C10100 (99.99% Cu), C10300 (99.95% Cu+10-50 ppm P), and C10800 (99.95% Cu+50–120 ppm P).

The microstructure was studied before testing in a light optical microscope (LOM). The microstructure of the various materials before testing can be found in Figure 2-1. The microstructure is very close for the different batches except when the grain size is varied.

Table 2-1. Material data for the extruded copper.

Material number*	Test series	Grain size (µm)	S (ppm)	P (ppm)	H_2 (ppm)	O_2 (ppm)
1	CuP0_300	300	6	< 1	< 0.5	1.1
2 (11)	CuP30_450	450	6	29	< 0.5	1.2
3 (14)	CuP60_350	350	6	58	< 0.5	1.1
4	CuP105_450	450	5	106	< 0.5	1.1
5	Cu65_450	450	12	67	< 0.5	1.1
6 (13)	CuP60_100	100	6	58	< 0.5	
7	CuP60_800	800	6	57	< 0.5	1.6
8	CuP60_2000	2000	6	62	< 0.5	1.3

* The numbers in brackets indicate that the same material was used in the recrystallization work reported in /1-7/.

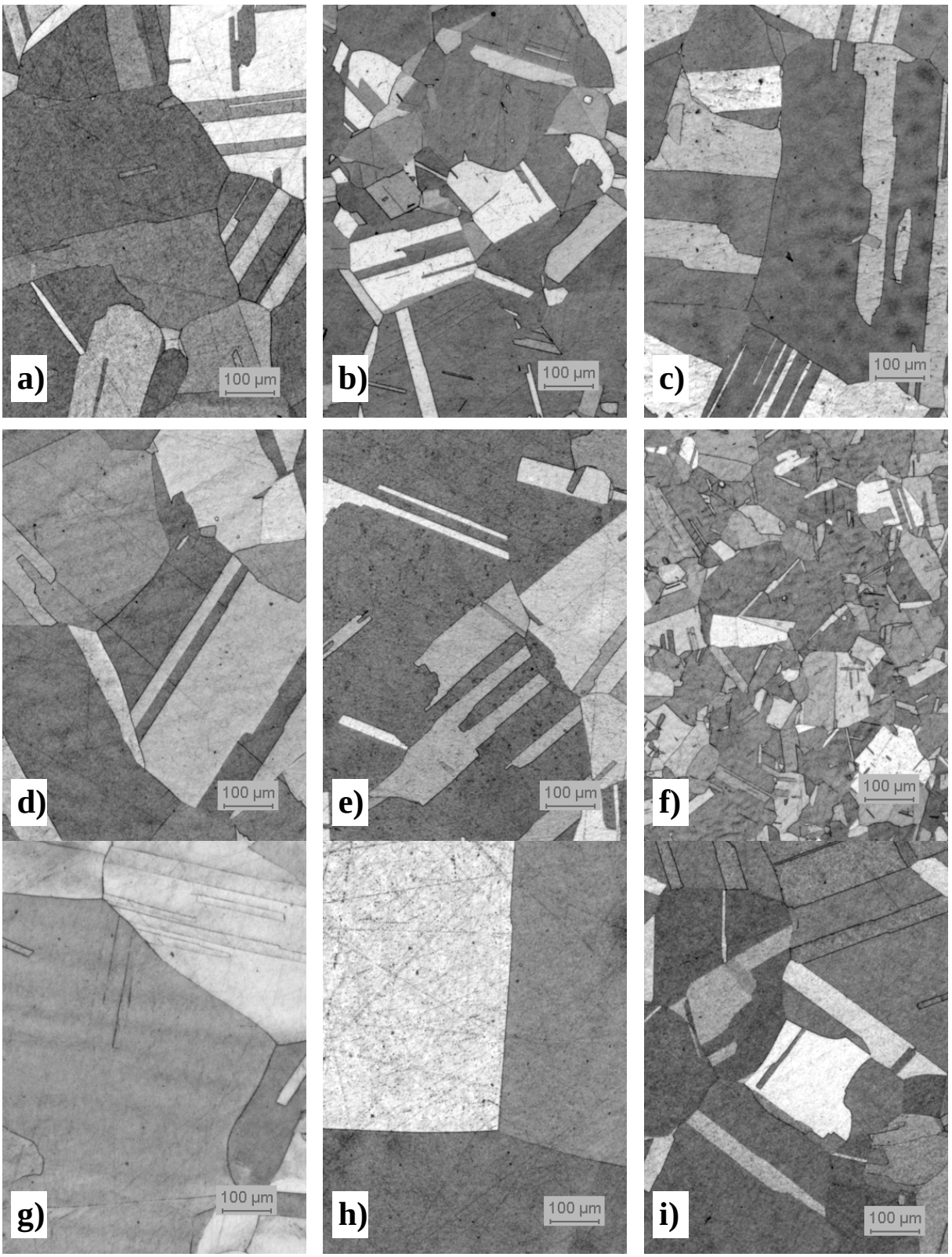

Figure 2- 1. *Microstructure in the material before creep testing. a) CuP0_300, b) CuP30_450, c) CuP60_350, d) CuP105_450, e) CuP65_450, f) CuP60_100, g) CuP60_800, h) CuP60_2000, i) CuP0_300 (second series). For material data see Table 2-1. LOM, 50x.*

Table 2-2. Tensile test data and hardness data.*

Test series	$R_{p0.2}$ (Mpa)	R_m (Mpa)	Elongation (%)	Hardness (HV)
CuP0_300	62	228	45	55
CuP30_450	**	**	**	53
CuP60_350	52	225	45	55
CuP105_450	51	224	46	***
Cu65_450	52	231	45	57
CuP60_100	56	231	46	55
CuP60_800	53	225	46	61
CuP60_2000	55	244	37	64

* Tensile tests were performed in room temperature with 10 mm diameter specimens and A5 gauge length. Hardness measurements were performed with 100 g micro-Vickers impression geometry.

** No data available for material CuP30_450.

*** No data available for material CuP105_450.

2.2 Creep testing

Standard uniaxial creep test specimens with a gauge diameter of 10 mm and a gauge length of 80 mm were machined from the extruded copper rods. Extra care was taken to avoid any cold working of the copper during machining. Testing was performed in uniaxial lever creep test rigs in air and the temperature was monitored by thermocouples attached to the gauge length. Strain was measured by extensometers attached to knife-edges on both sides of the gauge length.

When the displacement in a specimen reaches 5 mm (6% strain) the weight lever is close to the floor and the rig has to be reset. During this operation the specimen has to be temporarily unloaded, which means a redistribution of stresses. For tests with large strains several resets had to be made. The effect has been a renewed primary creep stage, see Figure 2-2. When this happened during primary or secondary creep stages the result was a slightly higher creep rate after the reset. However, if the specimen was in the tertiary creep stage when the machine had to be reset, the specimen tended to rupture shortly after or even during the reset. Creep life was thus shortened but since the specimens was already near creep rupture the influence has been minor for the creep testing as a whole.

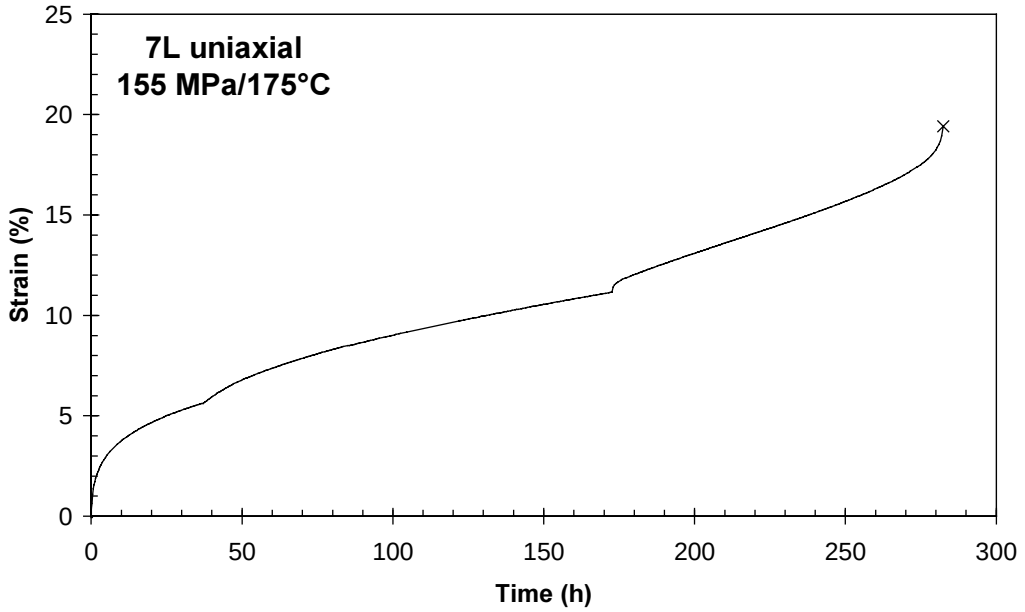

Figure 2-2. *Example of the renewed primary creep detected in specimens temporarily offloaded during resets of the creep machine.*

2.3 Metallography

Creep tested material was studied. The specimens were sectioned, mounted in cold setting resin, ground and finally polished. An etching agent consisting of ferric chloride was used.

3 Results

3.1 Test matrix

The creep test matrix can be found in Tables 3-1–3-3. At the time of writing 35 tests have been completed, 1 has been interrupted and 3 tests are still in progress. These last three have reached the minimum creep rate and are included in the results and discussion below.

Table 3-1. Creep test results. Influence of grain size.

Nominal grain size (μm)	Material number	Test series	Temp (°C)	Stress (MPa)	Rupture (h)	Min. creep rate (%h)	Creep strain (%)	Reduction in area (%)
100	6	CuP60_100	175	160	242	6.13×10^{-2}	40.7	84.7
				155	949	1.51×10^{-2}	38.3	69.1
				150	1486	1.06×10^{-2}	37.4	75.4
				145	Runn	1.13×10^{-3}	Runn	Runn
350	3	CuP60_350	175	160	240	4.53×10^{-2}	36.4	94.7
				155	231	5.08×10^{-2}	25.0	80.6
				155	103	1.42×10^{-1}	30.0	75.6
				150	2351	4.66×10^{-3}	32.1	71.4
				147.5	1173	1.11×10^{-2}	28.5	71.4
800	7	CuP60_800	175	160	60	8.86×10^{-2}	25.1	95.6
				155	283	2.90×10^{-2}	27.1	73.9
				152	510	1.52×10^{-2}	25.2	65.8
				150	8997	3.40×10^{-4}	20.1	45.9
2000	8	CuP60_2000	175	160	39	2.49×10^{-2}	9.8	49.3
				155	84	4.44×10^{-2}	12.0	61.9
				150	2138	1.72×10^{-3}	7.7	44.1
				145	67	4.00×10^{-2}	9.9	76.6
				120	5012	4.47×10^{-4}	9.3	57.3

Table 3-2. Creep test results. Influence of phosphorous variation.

P content (ppm)	Material number	Test series	Temp (°C)	Stress (Mpa)	Rupture (h)	Min. creep rate (%/h)	Creep strain (%)	Reduc-tion in area (%)
< 1	1	CuP0_300	175	150	5	1.49×10^{0}	10.4	43.4
(first				140	27	7.51×10^{-2}	8.2	35.9
series)*				135	24	2.00×10^{-1}	9.3	30.3
				130	29	6.87×10^{-2}	7.8	36.0
< 1	1b	CuP0_300	175	130	116	1.81×10^{-2}	7.7	17.9
(second				120	315	5.49×10^{-3}	6.6	35.8
series)*				110	675	2.60×10^{-3}	8.8	29.5
				100	Runn	1.21×10^{-4}	Runn	Runn
29	2	CuP30_450	175	160	92	7.00×10^{-2}	31.7	77.8
				150	147	3.62×10^{-2}	37.0	79.9
				147.5	676	1.24×10^{-2}	35.1	69.6
				145	11086	8.14×10^{-4}	25.8	56.4
58	3	CuP60_350	175	160	240	4.53×10^{-2}	36.4	94.7
				155	231	5.08×10^{-2}	25.0	80.6
				155	103	1.42×10^{-1}	30.0	75.6
				150	2351	4.66×10^{-3}	32.1	71.4
				147.5	1173	1.11×10^{-2}	28.5	71.4
106	4	CuP105_450	175	155	215	4.72×10^{-2}	25.8	75.3
				150	677	1.67×10^{-2}	26.9	80.7
				150	Runn	4.00×10^{-4}	Runn	Runn
				145	3169	3.60×10^{-3}	27.5	69.4

* The first series with a P content of less than 1 ppm yielded no test with a longer rupture time than 29 hours, so a second series was manufactured and tested at significantly lower stress levels.

Table 3-3. Creep test results. Influence of sulphur variation.

S content (ppm)	Material number	Test series	Temp (°C)	Stress (Mpa)	Rupture (h)	Min. creep rate (%/h)	Creep strain (%)	Reduc-tion in area (%)
6	3	CuP60_350	175	160	240	4.53×10^{-2}	36.4	94.7
			175	155	231	5.08×10^{-2}	25.0	80.6
			175	155	103	1.42×10^{-1}	30.0	75.6
			175	150	2351	4.66×10^{-3}	32.1	71.4
			175	147.5	1173	1.11×10^{-2}	28.5	71.4
12	5	CuP65_450	175	160	171	9.41×10^{-2}	29.7	83.1
			175	155	116	7.78×10^{-2}	29.8	84.0
			175	155	Interr	1.92×10^{-3}	Interr	Interr
			175	150	1032	6.25×10^{-3}	24.4	74.5
			175	145	6414	1.50×10^{-3}	36.8	61.2

3.2 Grain size variations

As can be seen from Figure 3-1, there are no significant difference in creep strength for the different grain sizes tested, with the exception of the largest tested grain size, 2000 µm (CuP60_2000), which exhibits a slightly lower creep strength. Time to 5% and 10% strain versus stress can be found in Figure 3-2 and Figure 3-3. These times show little variation with grain size except possibly for 2000 µm.

When a material is creep tested it usually exhibits a creep strain rate that is continuously decreasing in the early part of the testing, then constant during a part of the testing and finally increasing until final fracture. The constant creep rate portion of the test is called the steady state part and is characterised by exhibiting the minimum creep strain rate during the test. The minimum creep rate $\dot{\varepsilon}_{ss} = B\sigma^n$ can be expressed by the Norton equation (3-1).

$$\dot{\varepsilon}_{ss} = B\sigma^n \tag{3-1}$$

where B and n are constants and σ the stress. For the testing performed in this work high values of the Norton stress exponent, n, have been found. In Figure 3-4 the exponent takes values between 14 and 73 for the various tested materials. The test temperature is hence well inside the power law break-down area, and since the capsules are to operate at these stress levels the results are relevant. The ductility properties in Figure 3-5 and Figure 3-6 show an increasing creep rupture elongation with decreasing grain size with a maximum of about 40% for the specimens with 100 µm grain size (CuP60_100). The reduction in area is about the same for all tested grain sizes.

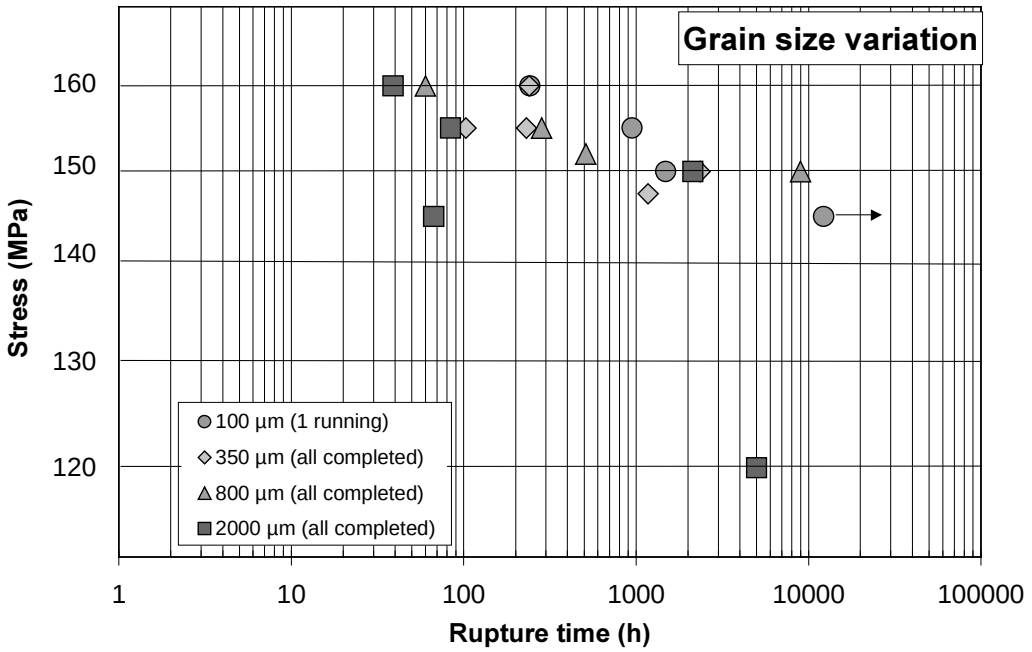

Figure 3-1. *Stress versus rupture time for specimens with varying grain sizes. Arrows denote tests still in progress.*

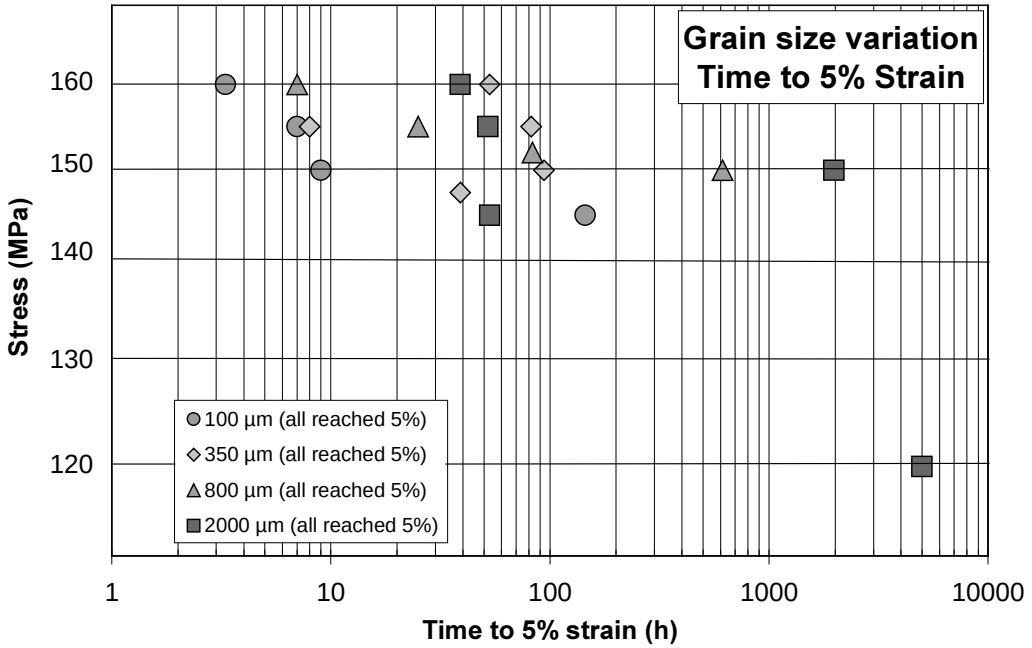

Figure 3-2. *Stress versus time to 5% strain for specimens with varying grain size.*

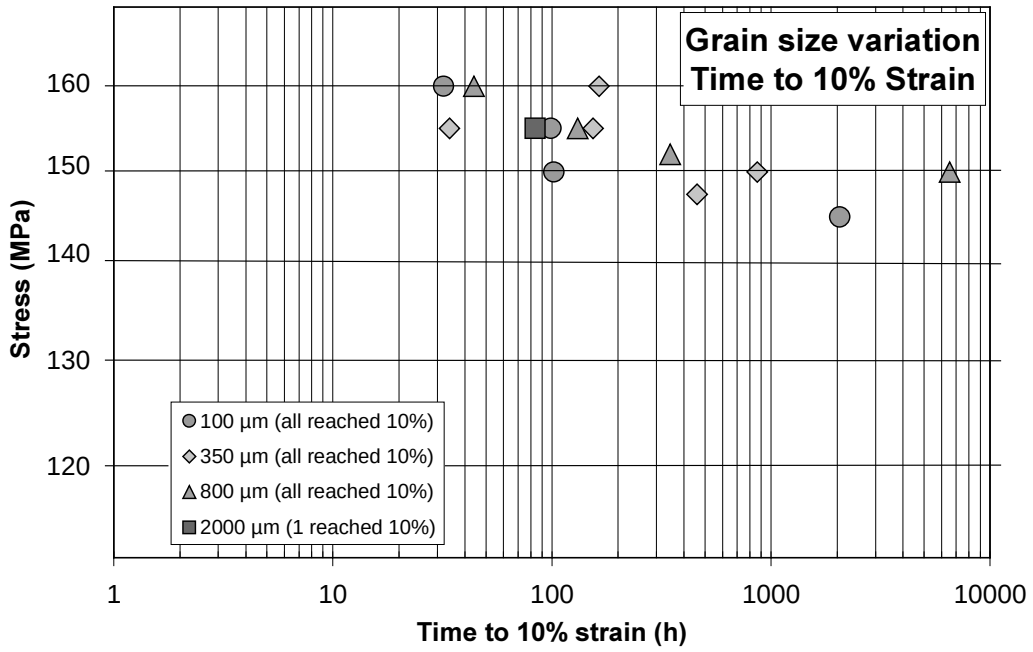

Figure 3-3. *Stress versus time to 10% strain for specimens with varying grain size.*

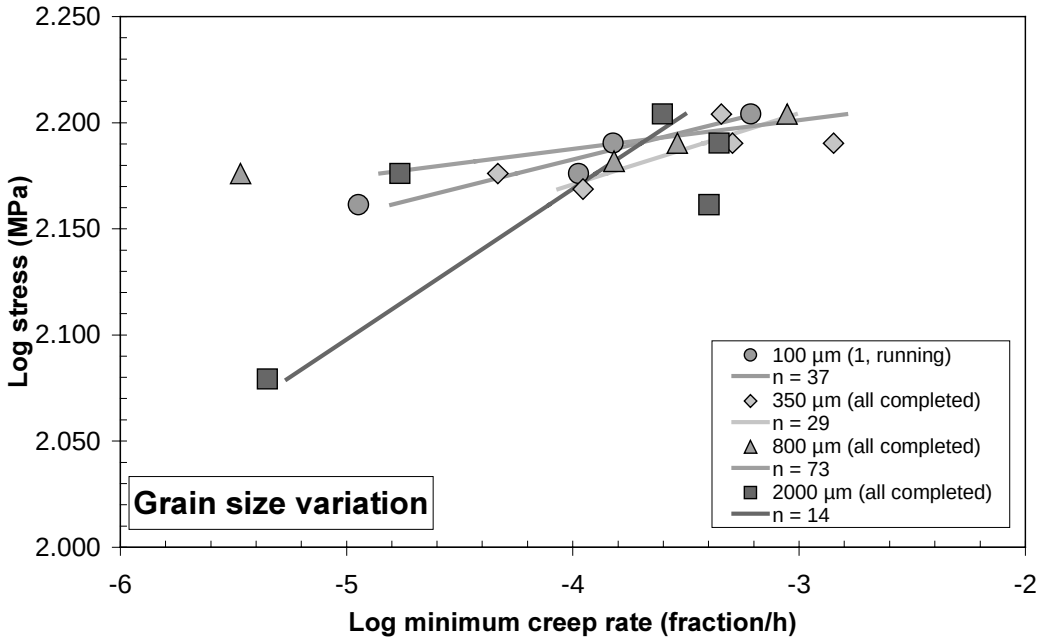

Figure 3-4. *Norton plot for the specimens with varying grain size. All specimens that have reached the minimum creep rate are included.*

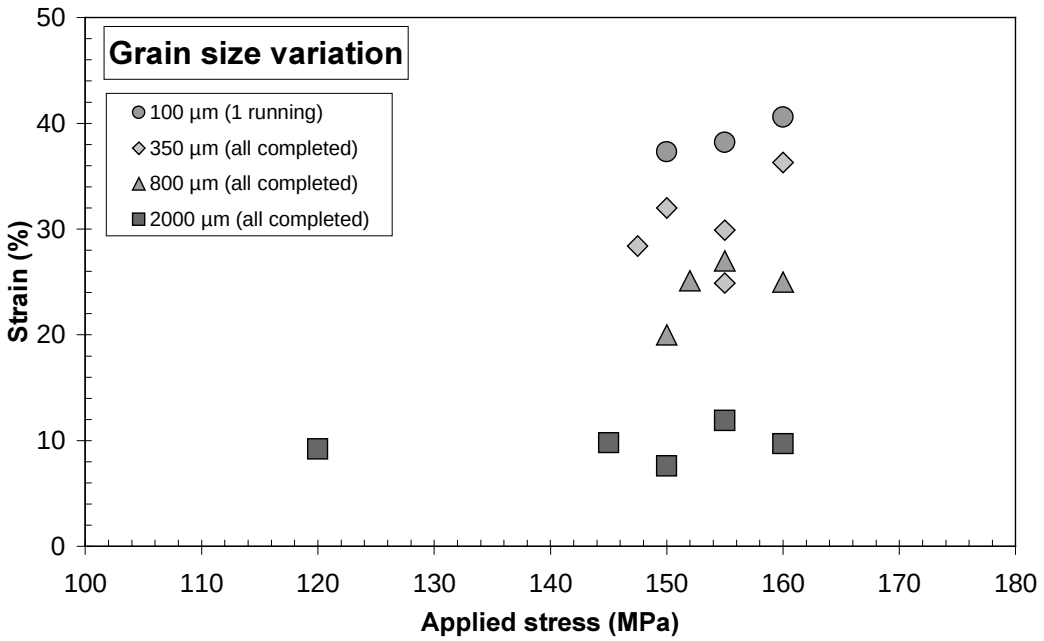

Figure 3-5. *Creep strain versus stress for specimens with varying grain size.*

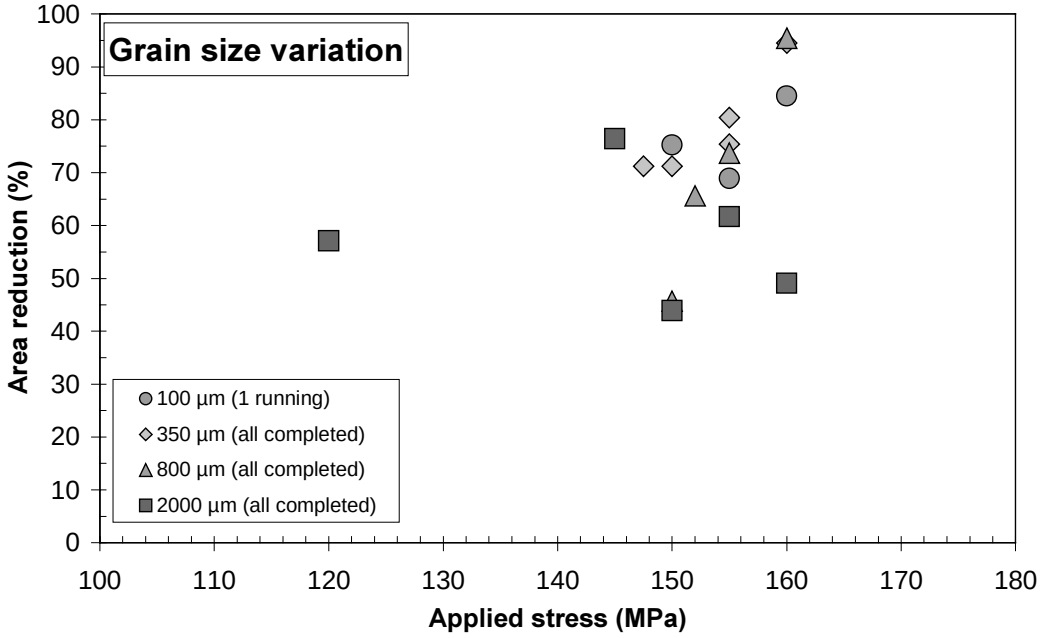

Figure 3-6. *Reduction in area versus stress for specimens with varying grain size.*

3.3 Sulphur variation

The variation in sulphur content did not have any noticeable effect on the creep properties, as can be seen from time to rupture versus stress in Figure 3-7, time to 5% strain versus stress and time to 10% strain versus stress in Figure 3-8 and Figure 3-9. The Norton exponent took values of 29 and 38, see Figure 3-10. The ductility measurements for elongation at rupture and reduction in area are presented in Figure 3-11 and Figure 3-12. No difference in the ductility between the batches is observed.

3.4 Phosphorous variation

Materials with four different phosphorous contents were creep tested. The stress – rupture plots can be found in Figure 3-13. It is evident that the material with the lowest phosphorous content (<1 ppm P, CuP0_300) has significantly lower creep rupture strength with rupture times up to two orders of magnitude lower at the same stress levels. Times to 5% and 10% strain can be found in Figure 3-14 and Figure 3-15. Shorter times are observed at lower P contents. The Norton exponent was determined to values between 21 and 38, see Figure 3-16. The exponent for the P-free copper is significantly lower than for the other batches. This material also exhibits a much steeper slope of the stress – rupture curve than the materials with higher phosphorous content leading to shorter rupture times at lower stress levels, see Figure 3-13. The creep rupture strain properties of the tested materials can be found in Figure 3-17 and Figure 3-18. The material with the lowest phosphorous content exhibits the lowest ductility properties with elongation lower than 10% whereas the other materials with higher phosphorous content all have rupture strains of about 30%. The same difference can be found in the reduction in area in Figure 3-18.

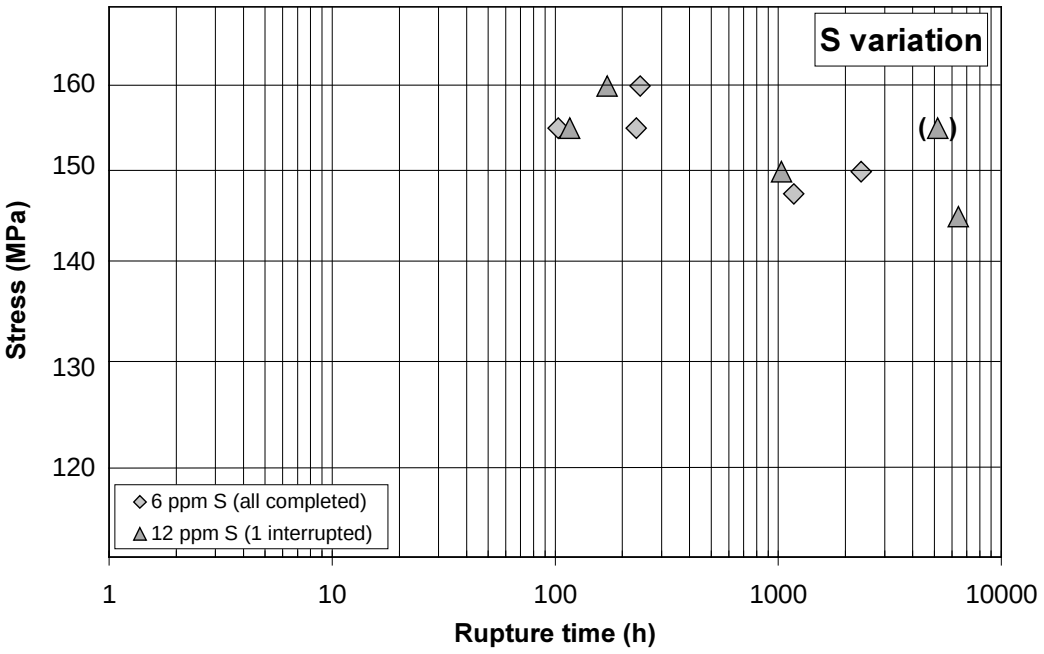

Figure 3-7. *Stress versus rupture time for specimens with varying sulphur content. One test was interrupted.*

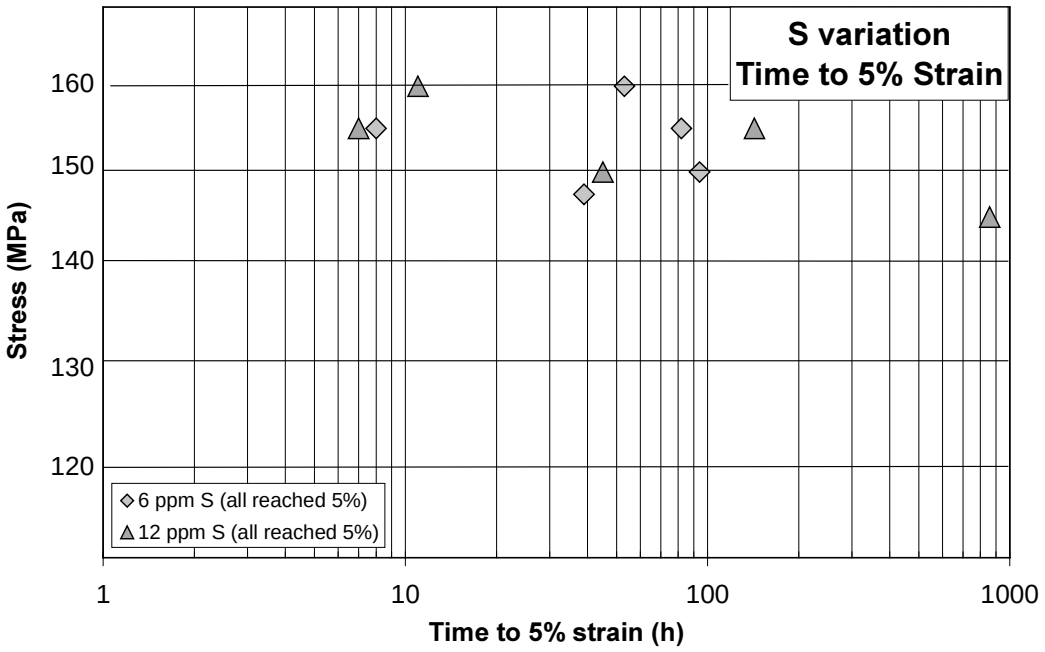

Figure 3-8. *Stress versus time to 5% strain for specimens with varying sulphur content.*

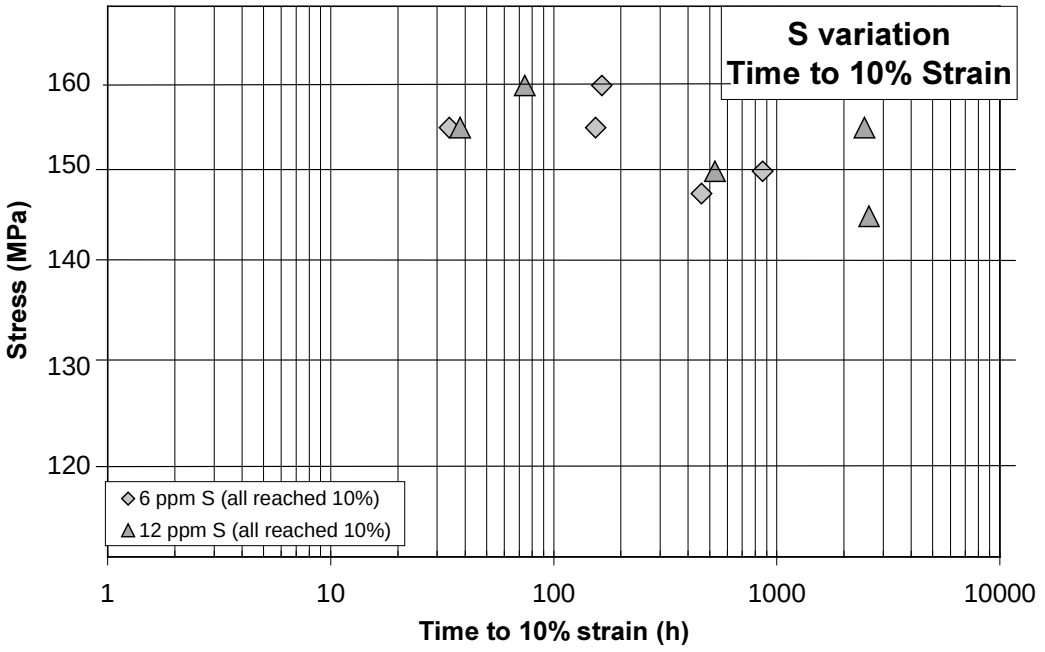

Figure 3-9. *Stress versus time to 10% strain for specimens with varying sulphur content.*

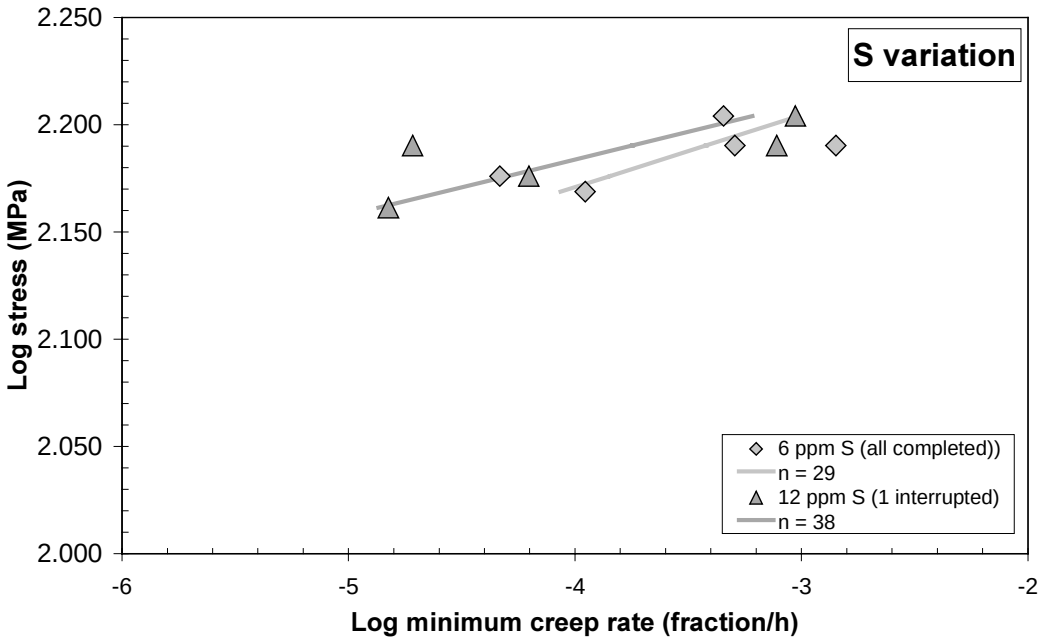

Figure 3-10. *Norton plot for the specimens with varying sulphur content. All specimens that have reached the minimum creep rate are included.*

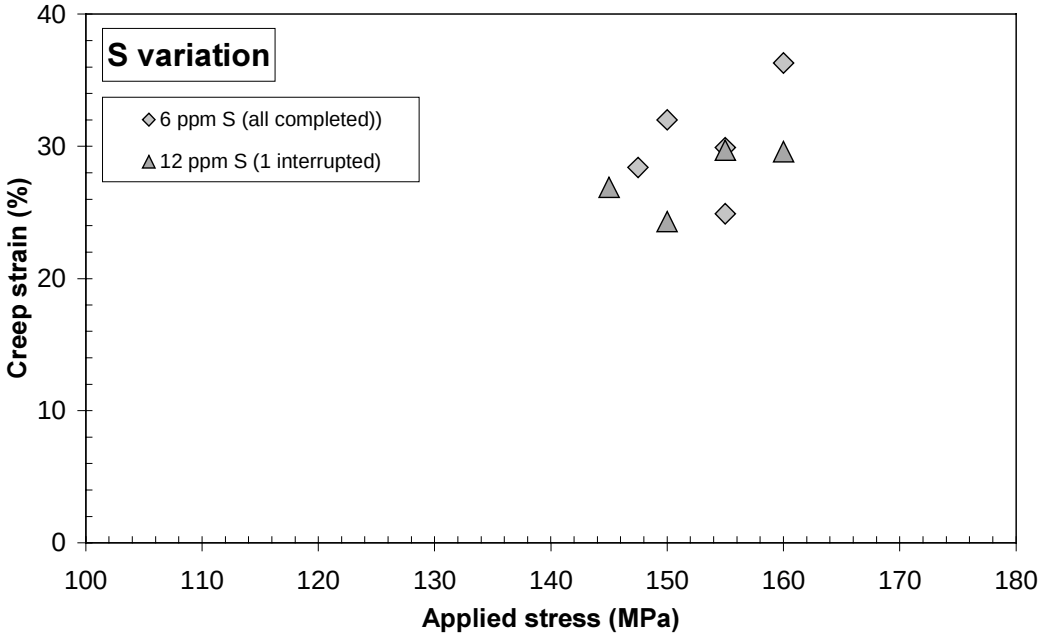

Figure 3-11*. Creep strain versus stress for specimens with varying sulphur content.*

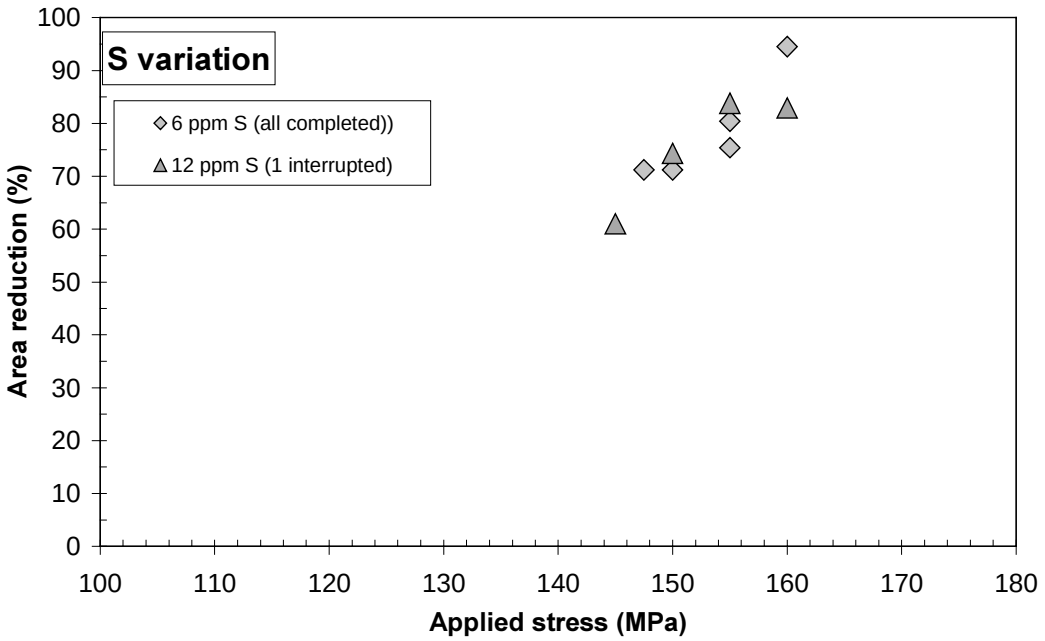

Figure 3-12. *Reduction in area versus stress for specimens with varying sulphur content.*

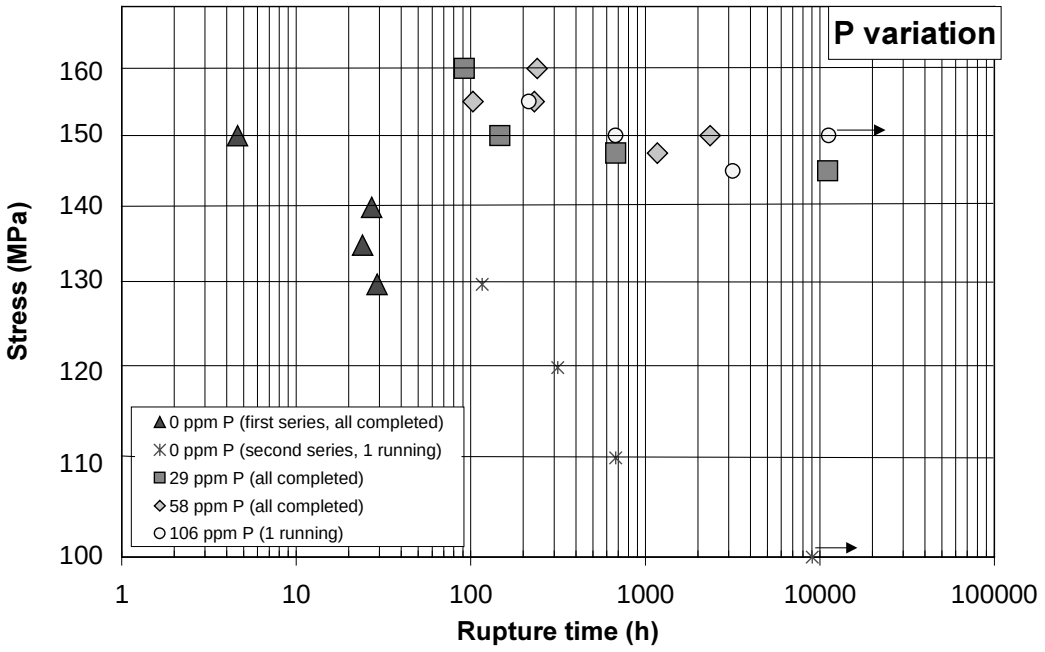

Figure 3-13*. Stress versus rupture time for specimens with varying phosphorous content. Arrows denote tests still in progress.*

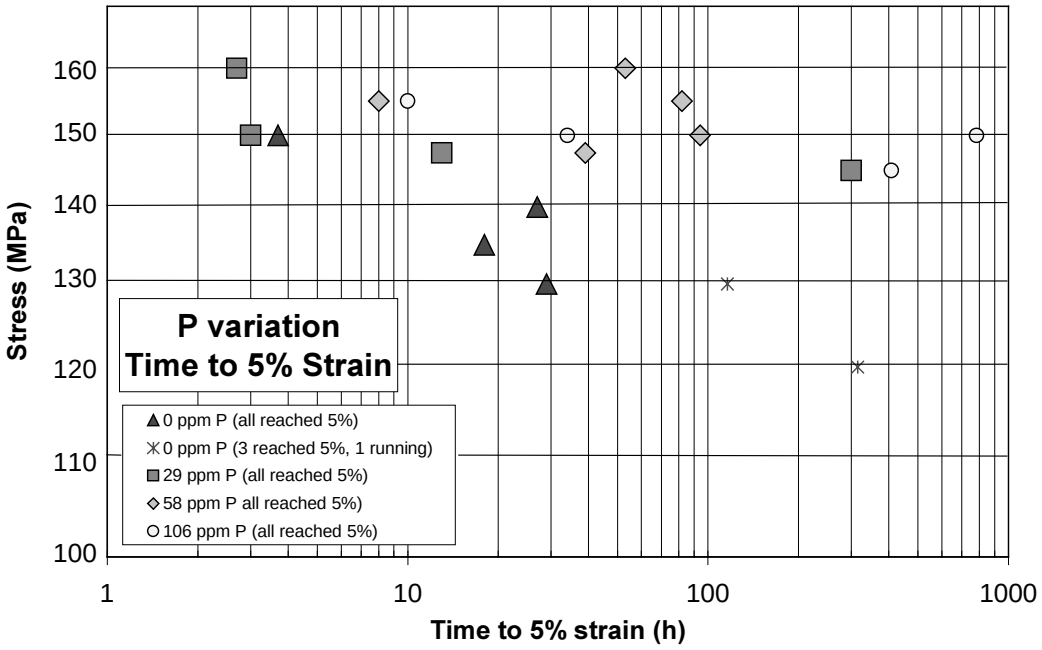

Figure 3-14. *Stress versus time to 5% strain for specimens with varying phosphorous content.*

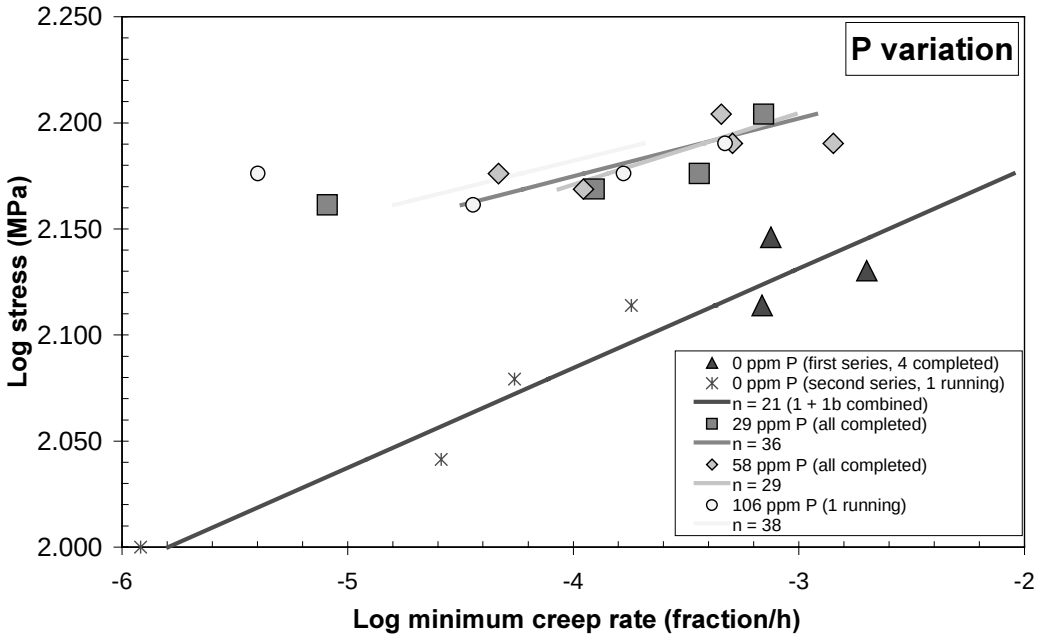

Figure 3-15. *Stress versus time to 10 % strain for specimens with varying phosphorous content.*

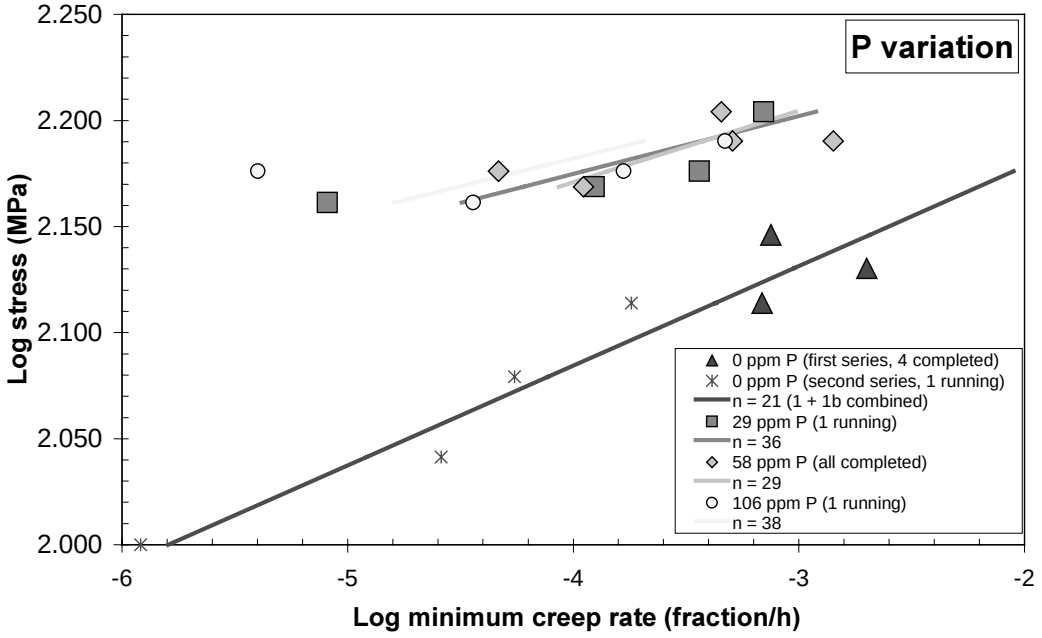

Figure 3-16. *Norton plot for the specimens with varying phosphorous content. All specimens that have reached the minimum creep rate are included.*

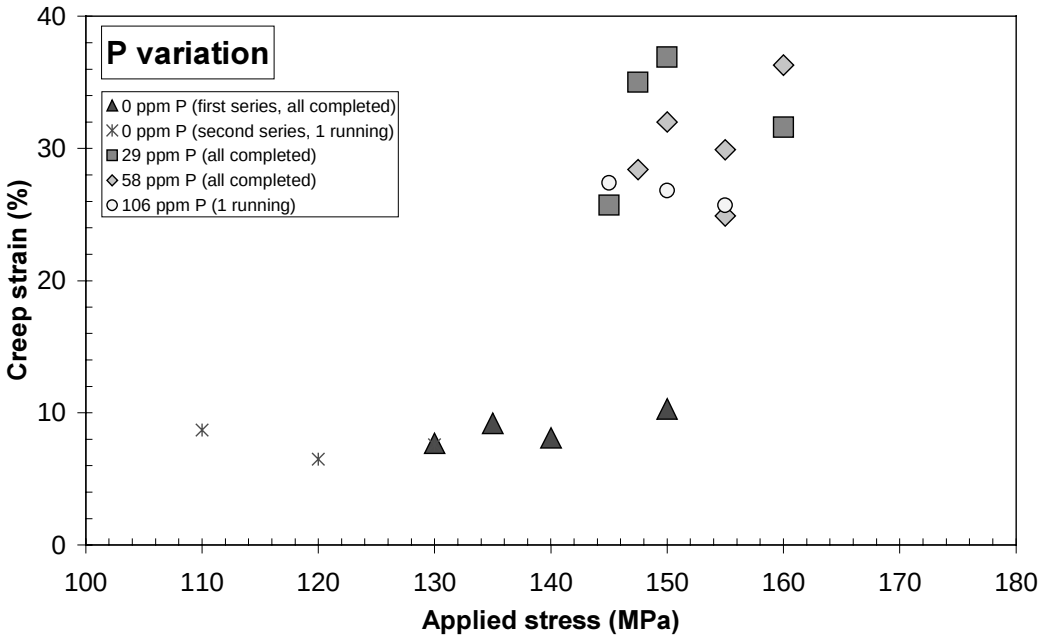

Figure 3-17. *Creep strain versus stress for specimens with varying phosphorous content.*

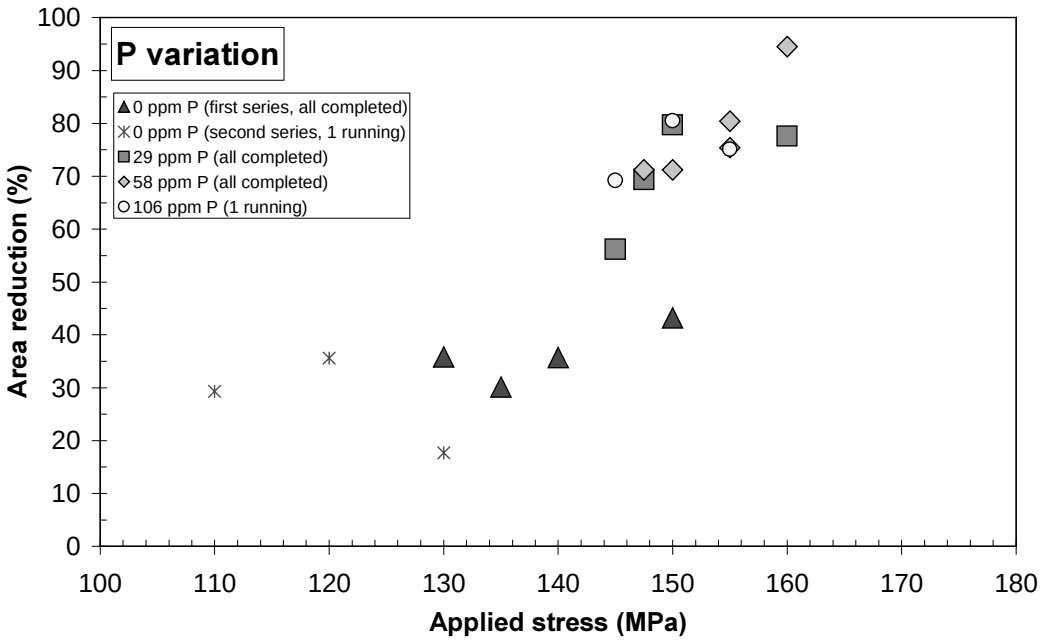

Figure 3-18. *Reduction in area versus stress for specimens with varying phosphorous content.*

3.5 Microstructure

The material with 100 µm grain size (CuP60_100) shows large amounts of cavities near the fracture, as well as large plastic deformation of the grains, see Figure 3-19. Further away from the fracture the cavity density decreases but cavities can be found throughout the gauge length. In the specimens with progressively larger grain sizes the evidence of cavitation disappears and instead microcracking is evident. In the 350 µm specimen (CuP60_350) linking of cavities can be seen, see Figure 3-20, but in the 800 (CuP60_800) and 2000 µm (CuP60_2000) specimens no cavities can be seen, just microcracks. Furthermore the microcrack density away from the fracture increases with grain size. In the 2000 µm copper microcracks with a length of up to 1000 µm can be observed at a distance of five times the specimen diameter from the fracture (50 mm). Triangular shaped microcracks (wedge cracks) are present at triple points even at distances far away from the fracture, see Figure 3-21.

The presence of sulphur does not seem to influence the fracture mechanism. The high sulphur batch also demonstrates linking of cavities leading to the formation of micro-cracks, see Figure 3-20 and Figure 3-22.

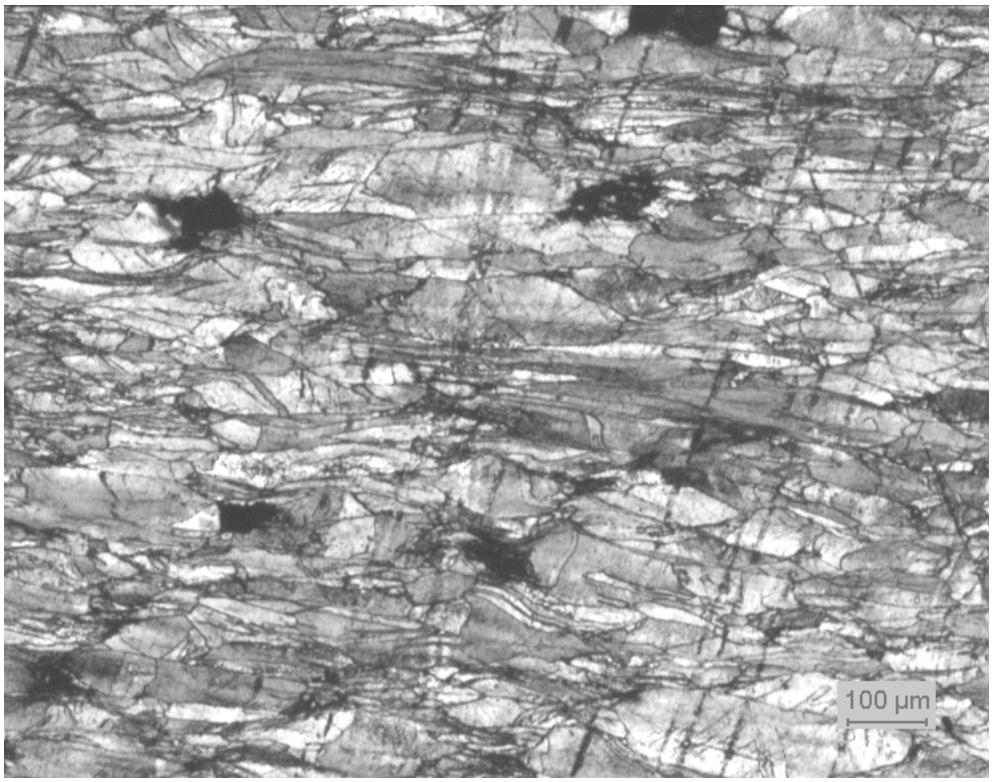

Figure 3-19. *Cavitation and plastic deformation close to the fracture in a specimen with 100 µm grain size (CuP60_100). Specimen 6J, 150 MPa, 175 °C, 1486 h. LOM, 50x.*

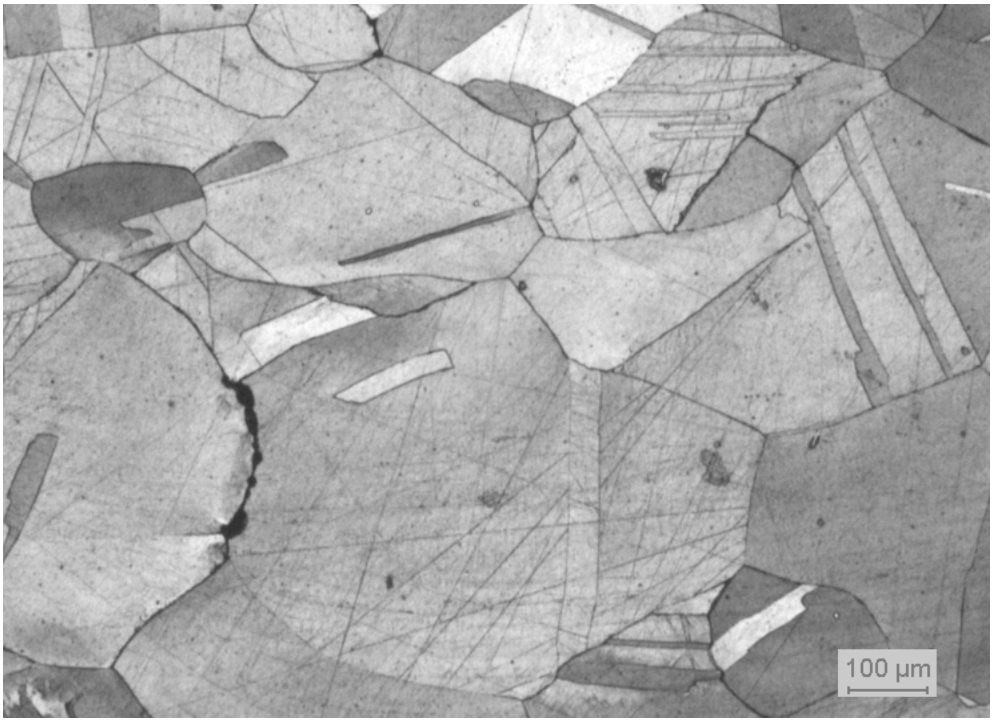

Figure 3-20. *Microcracks formed by linking of cavities 50 mm from fracture in a specimen with 350 µm grain size (CuP60_350). Specimen 3J, 150 MPa, 175 °C, 2351 h. LOM, 50x. (This is the reference material with 350 µm grain size, 6 ppm S and 58 ppm P).*

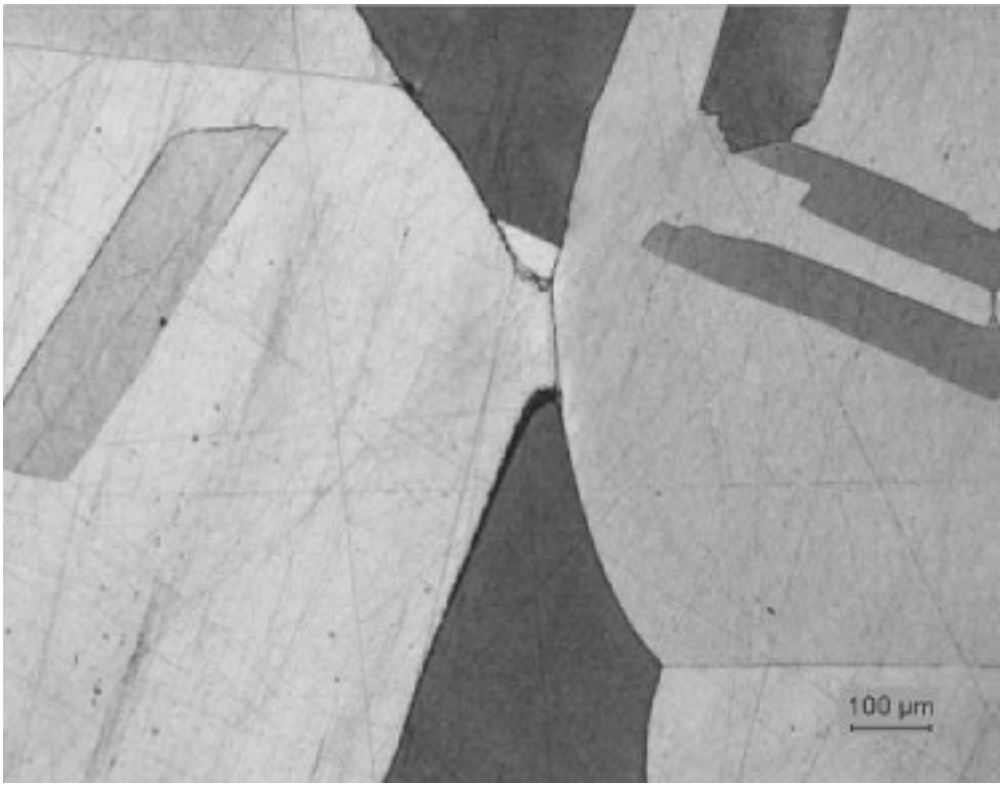

Figure 3-21. *Triangular shaped microcrack at a triple point 50 mm away from the fracture in a specimen with 2000 µm grain size (CuP60_2000). Specimen 8J, 120 MPa, 175 °C, 5012 h, LOM 50x.*

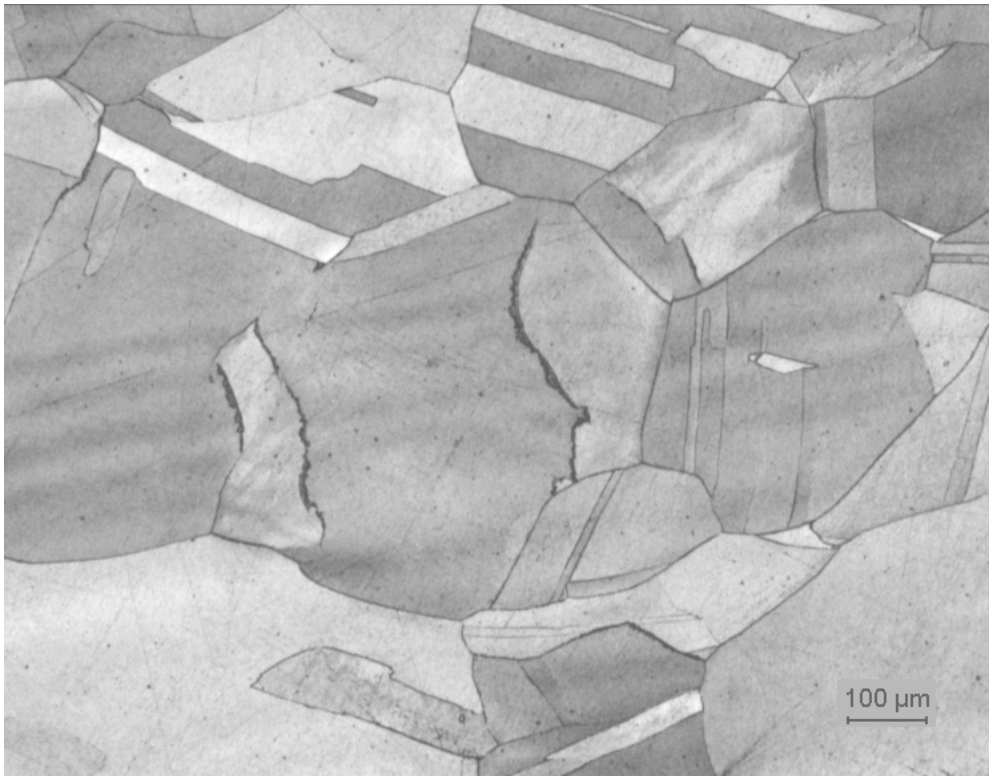

Figure 3-22. *Microcracks at a distance of 50 mm from the fracture in a specimen with 12 ppm S (CuP65_450). Specimen 5J, 150 MPa, 175 °C, 1032 h. LOM, 50x.*

In the material with the lowest phosphorous content (<1 ppm P, CuP0_300) the fracture is characterised by an absence of significant plastic deformation close to the fracture. Cavities and microcracks form throughout the material and wedge cracks can be found at triple points. The outer surface of the specimens is full of small, sharp microcracks (see Figure 3-23) and has a rather facetted appearance close to the fracture. These facets are probably the result of grain boundary sliding with little plastic deformation of the grains. Blunting of facets and the surface cracks in the specimens with higher phosphorous content, where the grains have experienced plastic deformation is obvious. In the materials with 29 ppm (CuP30_450) and 58 ppm (CuP60_350) phosphorous a shift from cavity formation to microcracks is evident. In a 58 ppm P specimen microcracks can be found in the whole gauge length, see Figure 3-20, and in the 29 ppm P specimen the defect location is the same but with shorter and less pronounced microcracks. The specimen with the highest phosphorous content (CuP105_450) shows a marked reduction of both the cavity and the microcrack density compared to the specimens with less phosphorous content. Few, if any, microcracks can be seen away from the fracture and the few surface cracks that can be observed are very blunt. The plastic deformation close to the fracture is large in this specimen.

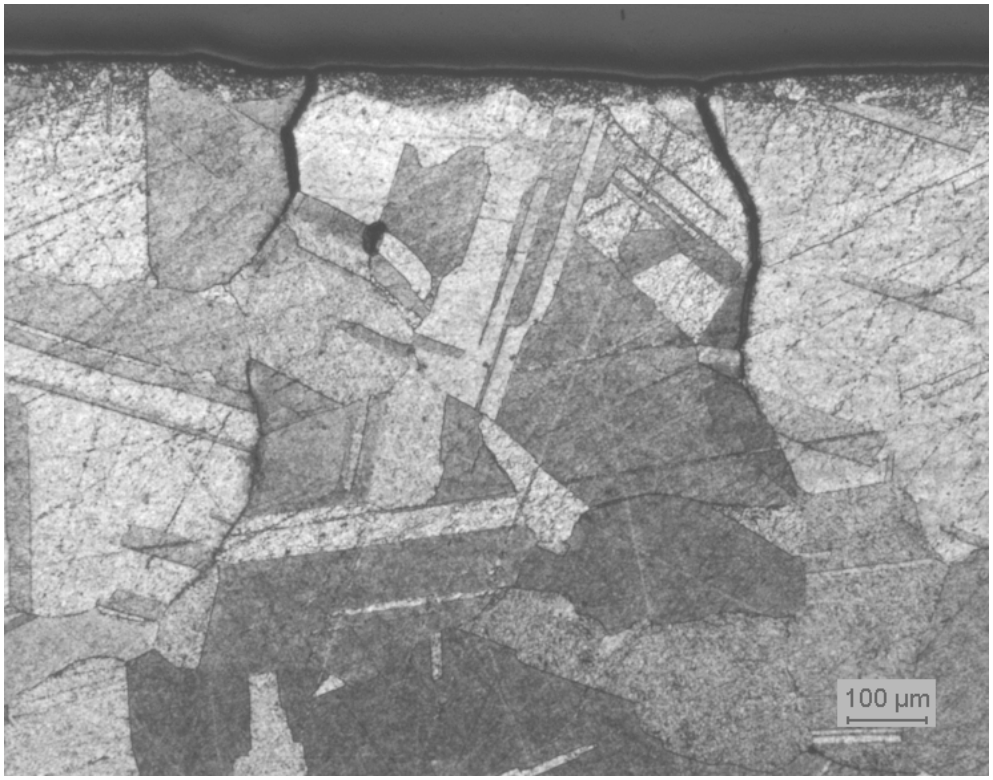

Figure 3-23. *Microcracks starting at the surface 50 mm from the fracture in a specimen with <1 ppm P (CuP0_300). Specimen 1Jb, 120 MPa, 175 °C, 315 h. LOM, 50x.*

4 Extrapolation of the creep rupture data

The data from four of the batches in the present investigation has been used for extrapolation namely CuP30_450, CuP60_350, CuP65_450, and CuP105_450. These batches have similar creep rupture data. This data has been combined with previously determined results for Cu-OFP from batches 400 and 500, /1-3, 1-5/. Data for all tests that have reached rupture is included in the analysis.

The Larson-Miller time temperature parameter

$$P_{LM} = T(\log t + C_{LM}) \tag{4-1}$$

where T is the temperature in K, t the time in h, and C_{LM} is a constant, has been used. A second order polynomial in P_{LM} has been fitted to the data at the same time as the value of C_{LM} was assessed. The resulting master curve is given in Figure 4-1 with a log scale and in Figure 4-2 with a linear scale. The new data can be found for P_{LM} < 6300. There are also two points from the previous investigations in this range. Extrapolation to 200 years at 75 and 100ºC in Figure 4-2 corresponds to P_{LM} values of 5800 and 6210 respectively, i.e. in the range of the new data. These are the expected exposure conditions in the repository. The corresponding rupture strength is in the interval 135 to 155 MPa.

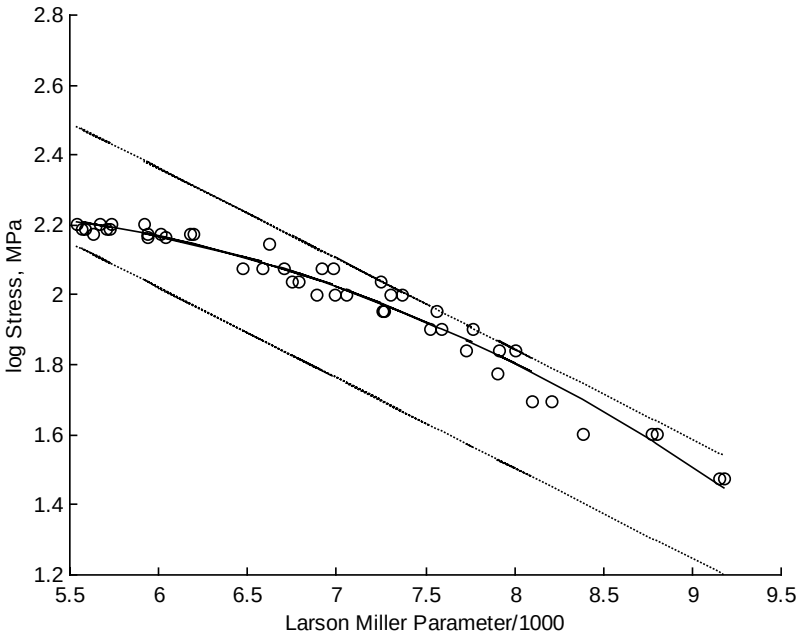

Figure 4-1. *Master curve for creep rupture extrapolation. Stress versus the Larson-Miller time temperature parameter. CuP30_450, CuP60_350, CuP65_450, and CuP105_450.*

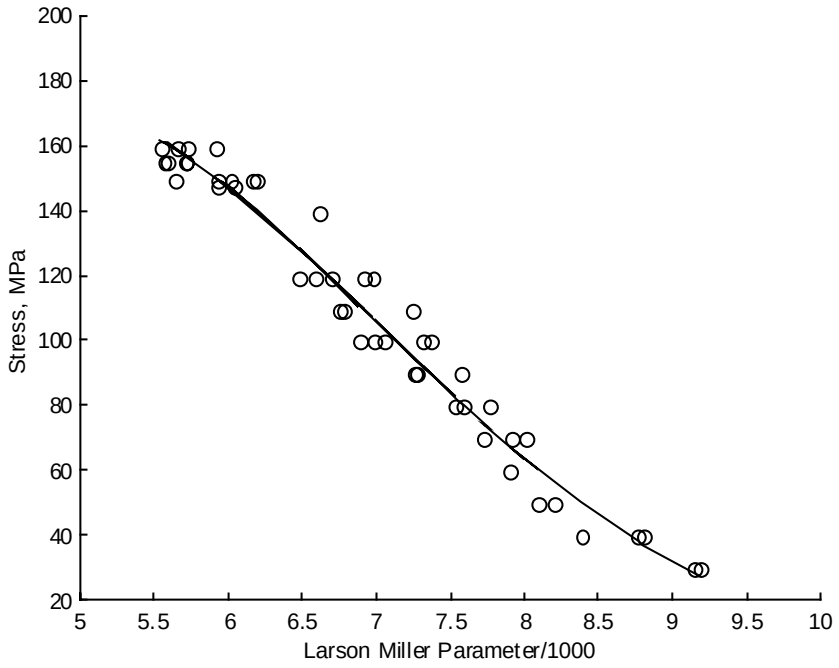

Figure 4-2. *Same as Figure 4-1 but with a linear scale.*

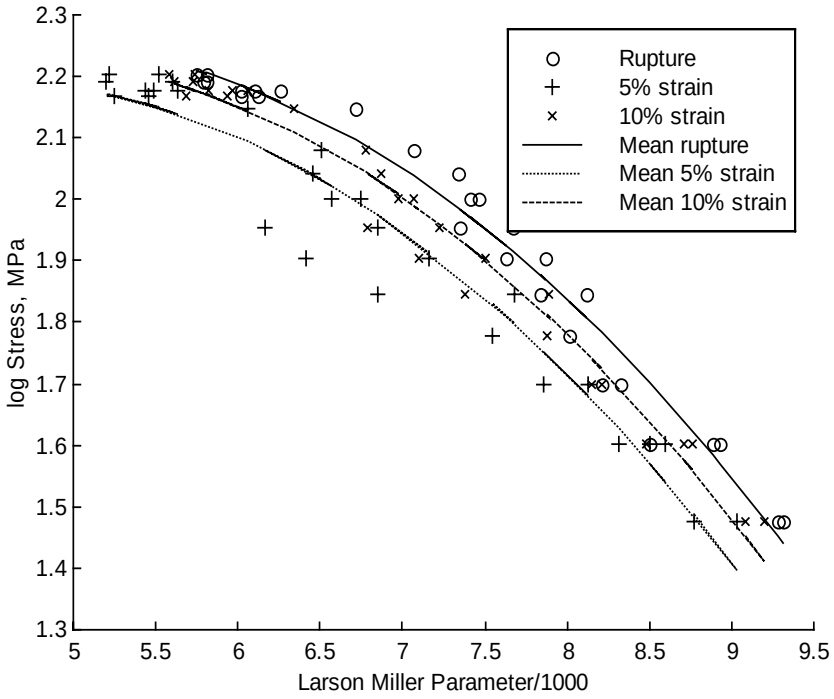

Figure 4-3. *Master curve for creep rupture, 5 and 10% strain extrapolation. Stress versus the Larson-Miller time temperature parameter. CuP30_450, CuP60_350, CuP65_450, and CuP105_450.*

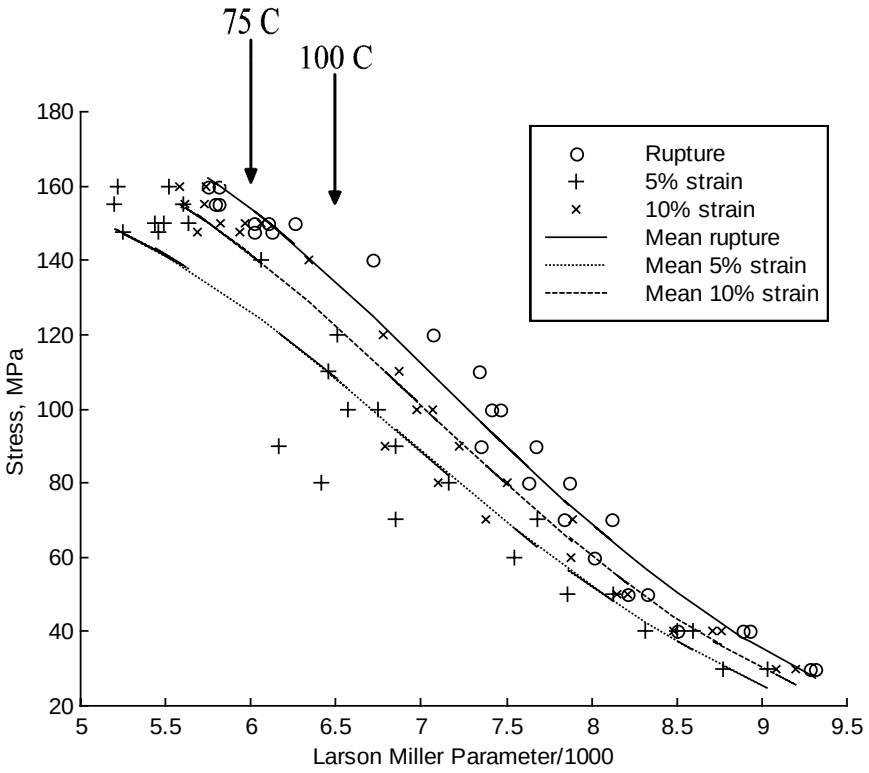

Figure 4-4. *Same as Figure 4-3 but with a linear scale. The estimated stresses giving rupture and 5 and 10% creep strain after 200 years at 75 and 100 ºC are marked with arrows.*

Extrapolation for the stresses to give 5 and 10% creep strain has also been carried out. A detailed discussion of the method used for extrapolating the results can be found in /4-1/. Instead of using a polynomial in stress, a polynomial in the Larson-Miller parameter has been applied. The resulting master curve is shown in Figure 4-3 and Figure 4-4 with different scales. Extrapolation to 200 years at 75 and 100 ºC gives stresses in the range 115 to 130 MPa and 130 to 145 MPa for 5 and 10% creep strain respectively.

5 Discussion

The tested materials have different grain size, sulphur content and phosphorous content. The tested materials exhibit ductility values over 20%, with the exception of the material with the largest grain size (CuP60_2000) and the material with no phosphorous content (CuP0_300) where the ductility is around 10% or less. These materials are also the only ones with significantly lower rupture times for the same applied stress than for the reference material.

The Norton exponents obtained in this work are larger than in previous investigations for P containing materials. In the present investigation values of about $n = 30$ have typically been found. This should be compared to $n = 5$ to 15 in previous work /5-1/. Since the testing in the present work has been performed at 175 ºC rather than at 225 ºC or above as in the earlier reports, such a change over is not surprising. It demonstrates that for P-containing coppers there a change in deformation mechanism at around 200 ºC. Above this temperature the deformation mechanism is power law creep. Below this temperature power law break down takes place.

Although there is little influence on tensile properties, the addition of 30–110 ppm P to pure copper reduces the creep rate and increases the rupture life dramatically. It has been known for a long period of time that phosphorous reduces the rates of the softening processes recovery and recrystallization of pure copper /5-2/. Climb rates of dislocations and the migration rates of grain boundaries are much reduced. The proposed mechanism is solute-drag, see for example /5-3/. This proposal is supported by recent estimates of the interaction energy between P-atoms and vacancies, which demonstrates that there is a strong interaction /5-4/. As a consequence P-atoms have a strong affinity to dislocation cores and grain boundaries, which reduces their mobility.

The creep rupture mechanism in materials with moderate grain sizes is cavitation at grain boundaries, leading to the formation of microcracks by linking. In the material with the largest grain size there is also evidence of wedge cracks at grain boundary triple points. It has previously been shown that the low creep ductility of P-free copper is due to segregation of sulphur, probably in the form of Cu_2S phase at the grain boundaries /1-2/. The mechanism for the positive effect of P on the creep ductility is still unknown. One proposal is that S and P compete about the vacancy positions at the grain boundaries since both elements show a strong element-vacancy interaction /5-4/.

6 Conclusions

- The largest grain sizes tested (800, 2000 µm) showed a decrease in creep ductility in relation to the reference grain size (300 µm). The largest grain size also gave reduced creep strength.
- An addition of 29 ppm phosphorous increased the creep strength and creep ductility significantly in comparison to P-free material. Further additions of phosphorous had little effect.
- Sulphur contents of 6 to 12 ppm gave no difference in creep properties.
- Norton exponents are high for all tested materials (14 to 73).

7 Acknowledgements

This project was entirely funded by SKB AB. Outokumpu Poricopper OY supplied the test material and performed the grain size measurements and the tensile tests.

References

Chapter 1

1-1 **Werme L, 1998.** Design criteria for canisters for spent nuclear fuel. SKB R-98-08, Swedish Nuclear Fuel and Waste Management Co.

1-2 **Henderson P J, Sandström R, 1998.** Low temperature creep ductility of OFHC copper. Materials science and engineering, A246, pp. 143–150.

1-3 **Seitisleam F, Henderson P J, Lindblom J, 1996.** Creep of copper for nuclear waste containment – Results of creep and tensile tests on Cu-OF, Cu-OFP, cathode copper and welded joints. Swedish Institute for Metals Research, Report IM – 3327.

1-4 **Henderson P J, 1994.** Creep of copper. International Seminar on Design and Manufacture of Copper Canisters for Nuclear Waste, Sollentuna, Sweden.

1-5 **Henderson P J, Werme L, 1996**. Creep testing of copper for radwaste canisters. Materials and Nuclear Power, EUROMAT 96, Bournemouth, United Kingdom.

1-6 **Andersson C-G, 1998.** Test manufacturing of copper canisters with cast inserts. SKB TR-98-09, Swedish Nuclear Fuel and Waste Management Co.

1-7 **Siwecki T, Petterson S, Blaz L, 1999.** Modelling of microstructure evolution and flow stress behaviour in association with hot working of Cu-P alloys. Swedish Institute for Metals Research, Report IM-1999-513.

1-8 **Hamzah S, Stålberg U, 1999.** Grain size as influenced by process parameters in copper extrusion. To be published.

Chapter 2

2-1 ASTM E112-88, 1988.

Chapter 4

4-1 **Sandström R, 1999.** Extrapolation of creep strain data for pure copper. Journal of Testing and Evaluation, JTEVA, Vol. 27, No. 1.

Chapter 5

5-1 **Sandström R, 1999.** Expert system on creep in copper, under development.

5-2 **Hutchinson W B, Ray R K, 1979.** Influence of phosphorus additions on the annealing behaviour of cold-worked copper. Metals Science, 125–130.

5-3 **Pettersson K, 1996.** A study of recrystallization in copper. Materials Research Centre, Report TRITA-MAC-0594.

5-4 **Korzhavyi P A, Abrikosov I A, Johansson B, 1999.** Theoretical investigation of sulfur solubility in pure copper and dilute copper-based alloys. Acta mater., Vol 47, No 5, pp. 1417–1424.